論 文
48A - 11 - 7

Two-Module TCSC의 운전모드 특성 연구

A Study on the Operating-Mode Characteristics of Two-Module Thyristor Controlled Series Compensator

鄭 敎 範*
(Gyo-Bum Chung)

Abstract - This paper aims at investigating the operating-mode characteristics of two-module Thyristor Controlled Series Compensator (TCSC) as an equivalent of the multi-module TCSC in a simple three-phase power transmission system. The load flow program is developed to analyze the steady-state characteristics of two-module TCSC system and to find the thyristor firing angles for the required real power flow. The stability calculation program is developed with Poincare mapping theory. Simulation studies of the TCSC power transmission system using EMTP are performed to evaluate the transient characteristics of two-module TCSC as a real power flow controller and to prove the results of the load flow calculation and the stability analysis. In the process of the study, the operating-mode characteristics of two-module TCSC are evaluated and compared to those of single-module TCSC.

Key Words : TCSC, Two-module TCSC, Multi-module TCSC, Vernier mode, Blocked mode, Full conduction mode

1. Introduction

Thyristor-Controlled Series Compensator (TCSC) can improve the power transfer capability of a power transmission system, damp the real power flow oscillation and compensate the impedance of the transmission line from capacitive range to inductive range[1]. A TCSC module consists of a series capacitor and parallel paths with a thyristor switch and a surge inductor, a metal-oxide varistor for overvoltage protection and a bypass breaker. The operating modes of a single module TCSC in a power transmission system are classified into the full conduction mode, the Vernier mode, and the blocked mode[1]. TCSC in the blocked mode has no gate signals of thyristors and zero thyristor conduction. TCSC in the full conduction mode has continuous gate signals of thyristors. TCSC in Vernier mode has the phase control of gate signals of thyristors and consequent partial thyristor conduction.

A complete TCSC power transmission system may be comprised of several such modules in series to improve power system performance[1,2]. The operating modes of the multi-module TCSC are the combination of the full conduction mode, the Vernier mode and the blocked mode. Using two-module TCSC power transmission system shown in Fig. 1, the approximate equivalent of operating modes of the multi-module TCSC in a power transmission system can be obtained.

In order to investigate the operating-mode characteristics of two-module TCSC in a simple power transmission system, the load flow calculation, the stability analysis and EMTP simulations are performed for the combinations of the blocked mode and the Vernier mode and of the full conduction mode and the Vernier mode with emphasis on power flow control. Comparison between the characteristics of operating modes of a single module TCSC and those of operating modes of a two-module TCSC are also made. Appendix 1 shows the parameters of the TCSC power transmission system in Fig. 1.

2. Load Flow Calculation

Fig. 2 shows the relation between the thyristor conduction angle of TCSC module and the compensated real power flow supplied by the system voltage E_1 in Fig. 1. The power flow controlled by TCSC depends on the thyristor conduction angle of TCSC modules, which is determined by the gate-firing angle and the power system parameters.

In order to find the gate-firing angles of thyristors, the power flows and the voltages in the TCSC power transmission system, which are essential for the evaluation

* 正 會 員 : 弘益大 電氣工學科 助敎授 · 工博
接受日字 : 1999年 4月 27日
最終完了 : 1999年 10月 21日

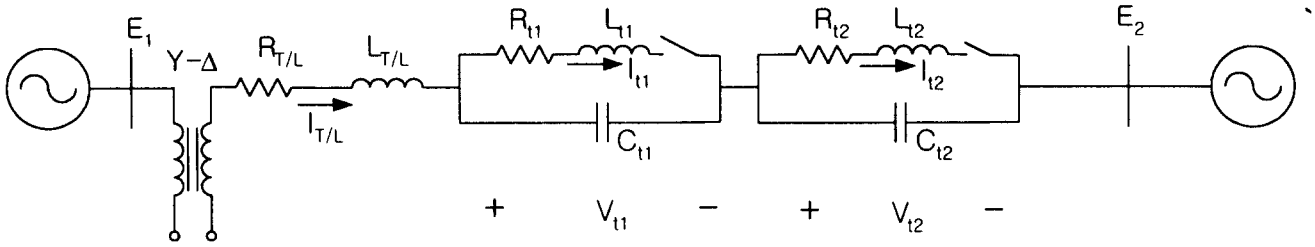

Fig. 1 The simplified single-phase diagram of a power transmission system with two-module TCSC

of the steady-state performance, the load flow calculation is performed.

For the load flow calculation, the switching function, $H_l(\omega t)$, describing the thyristor on/off states of the TCSC module 1, is used, which has a value of one when a thyristor is on and zero when the thyristor is off [3,4,5]. The complex Fourier series representation of the switching function, $H_l(\omega t)$, is

$$H_l(\omega t) = \sum_{n=-\infty}^{\infty} h_{l,n}(\sigma_l, \phi_l)\, e^{jn\omega t} \tag{1}$$

where $h_{l,n}$ is a function of the thyristor conduction angle σ_l, and the gate firing instant ϕ_l [3].

The capacitor voltage of TCSC module 1, $V_{tl}(\omega t)$, expressed in the complex Fourier series is

$$V_{tl}(\omega t) = \sum_{n=-\infty}^{\infty} V_{tl,n}\, e^{jn\omega t} \tag{2}$$

The inductor current of TCSC module 1, $I_{tl}(\omega t)$, expressed in complex Fourier series is

$$I_{tl}(\omega t) = Y_{tl} H_l(\omega t)\, V_{tl}(\omega t) \tag{3}$$

where Y_{tl} is the admittance matrix of the TCSC inductance branch. With the Thevenin's equivalent impedance matrix of the power transmission system except TCSC modules, Z_{TH}, and the admittance matrix of the TCSC capacitance branch, Y_{cl}, the terminal voltage of TCSC module 1, V_{tl}, is written as

$$V_{tl} = (Y_{tl} \cdot H_l + Y_{cl})^{-1} \cdot I_{T/L} \tag{4}$$

where the transmission line current I_{TL}, is

$$I_{T/L} = \frac{E_1 - E_2}{[Z_{TH} + (Y_{t1}H_1 + Y_{c1})^{-1} + (Y_{t2}H_2 + Y_{c2})^{-1}]^{-1}} \tag{5}$$

Then the real power flow, P_l, supplied by the system voltage E_l in Fig. 1, is written as

$$P_l = Re(3 \cdot E_l^*(wt) \cdot I_{T/L}(wt)) = g(\sigma_1, \phi_1, \sigma_2, \phi_2) \tag{6}$$

where E_l^* is the conjugate of E_l. If the values of σ and Φ in Eq. (6) were known, the real power flow, P_l, the harmonic voltage vector V_t and the current vector I_t can be easily found.

For the control scheme of the TCSC power transmission system, an equidistant firing and constant σ controller is used [3]. To find the values of σ_1, Φ_1 for the first module and σ_2, Φ_2 for the second module, two additional equations are derived from the condition that the thyristor currents are zero at the turn-off instants. The two constraint equations are written as

$$I_{t1}(\phi_1 + \sigma_1) = 0, \qquad I_{t2}(\phi_2 + \sigma_2) = 0 \tag{7}$$

With the Bisection method in numerical methods, the thyristor gate-firing angles ϕ_1 and ϕ_2 can be found simultaneously for a given value of the real power flow vector, P_l, of Eq. (6) [5]. Appendix 2 shows the results of the load flow calculation of the TCSC power transmission system in Fig. 1.

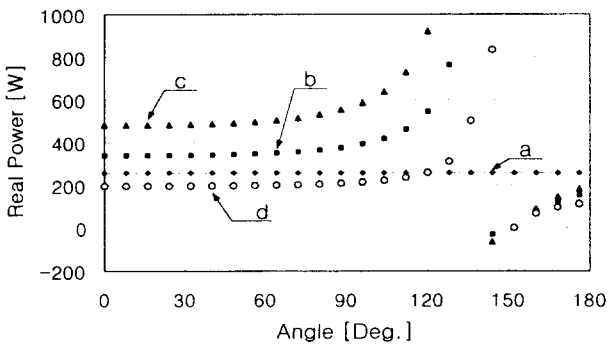

Fig. 2 The real power flow, P_l , versus the thyristor conduction angle σ [a : No compensation, b : Single Vernier mode, c : Vernier mode + Blocked mode, d : Vernier mode + Full conduction mode]

3. Stability Analysis

The stability analysis of two-module TCSC power

transmission system at different operating-mode is performed using the Poincare mapping from nonlinear dynamical systems theory[6]. The system state vector X(t) of the combined operation of a blocked mode TCSC module and a Vernier mode TCSC module is written as

$$X(t) = [\, I_{T/L}(t),\ I_{t2}(t),\ V_{t2}(t),\ V_{t1}(t)\,]^T \qquad (8)$$

During the conduction time of thyristors of the Vernier mode TCSC module, the system dynamics are described by the following set of linear differential equations:

$$\frac{dX(t)}{dt} = A \cdot X(t) + B \cdot E(t) \qquad (9)$$

where A is the system matrix and B is the constant matrix, shown in Appendix 3.

During the off state of thyristors of the Vernier mode TCSC module, the system dynamics are expressed as

$$\frac{dX(t)}{dt} = P_{rjt} \cdot A \cdot X(t) + P_{rjt} \cdot B \cdot E(t) \qquad (10)$$

where P_{rjt} is the projection matrix for the off state of thyristors of the Vernier mode TCSC module[3,4,5].

From the Poincare mapping theory, the stability of the TCSC power transmission system depends on the eigenvalues of the Jacobian Df, which is defined as

$$Df(X_0,\ \psi_1) = (e^{P_{rjt} \cdot A \cdot (\frac{T}{2} - \sigma_1)} \cdot P_{rjt} \cdot e^{A\sigma_1})^2 \qquad (11)$$

For the stable operation, the eigenvalues of Df lie inside the unit circle.

The stability analysis of the combined operation of the full conduction mode TCSC module and the Vernier mode TCSC module is similarly proceeded. Appendix 4 shows the system matrix, A and the constant matrix, B for the combined operation of the full conduction mode TCSC module and the Vernier mode TCSC module.

Fig. 3(a) shows the magnitude of the eigenvalues versus the thyristor conduction angle of the single-module TCSC power transmission system. The single module operation is stable over the full range of the conduction angle. Fig. 3(b) shows the magnitude of the eigenvalues of the combined operation of a Vernier mode TCSC module and a blocked mode TCSC module. Fig. 3(c) shows the magnitude of the eigenvalues of the combined operation of a Vernier mode TCSC module and the full conduction mode TCSC module. The maximum magnitude of the eigenvalues of two-module operations is less than 1, which means the TCSC power transmission system stable.

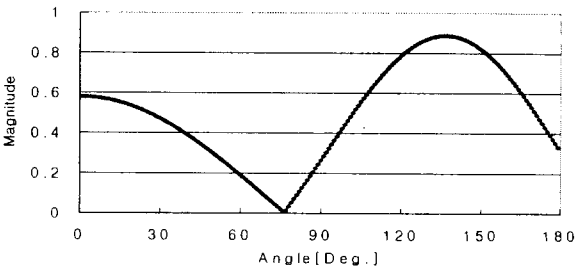

(a) Single module

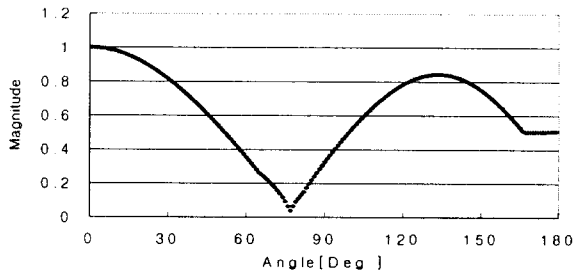

(b) Vernier mode + Blocked mode

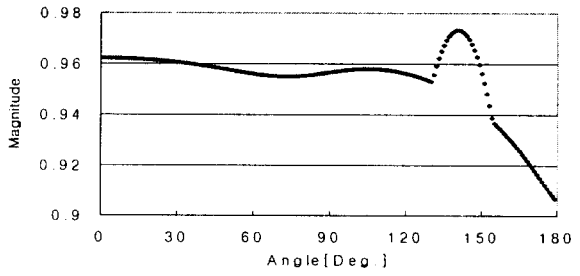

(c) Vernier mode + Full conduction mode

Fig. 3 The magnitude of the eigenvalues versus the thyristor conduction angle σ.

4. EMTP Simulation Study

The investigation of the operating-mode characteristics of the two-module TCSC power transmission system is performed with the computer simulation using EMTP. The EMTP simulation study includes the individual representation of thyristors, three-phase Y-Δ transformer, voltage sources and other circuit components, as well as the various control functions and signal processing elements for the control of TCSC module.

The system is initially operating without compensation and transmitting P_o=257[W] and Q_o=503[Var] at 40° phase angle difference from E_1 bus to E_2 bus in Fig. 1.

Fig. 4(a) shows the capacitor voltage, the reactor current and the transmission line current of the single module TCSC system with the phase angle of gate firing signal, φ=169.7° , obtained by the load flow calculation,

and the conduction angle σ=80° , transmitting P_{comp}=369.2[W] and Q_{comp}=637[Var]. Fig. 4(a) shows that the phase of the capacitor voltage of TCSC lags the T/L current by 90° , so the effective impedance of the TCSC module is capacitive. Fig. 4(b) and Fig. 4(c) show the transient performance of the power flows caused by the single-module TCSC insertion. The real power flow from the voltage source E_1 to the voltage source E_2 changes quickly and smoothly to its new power level, and the overshoot is well damped quickly, which is predicted by the eigenvalues in Fig. 3(a). The steady-state performance of the TCSC power transmission system in EMTP simulation, using the phase angle of gate-firing signals obtained by the load flow calculation, agrees with the results of the load flow calculation.

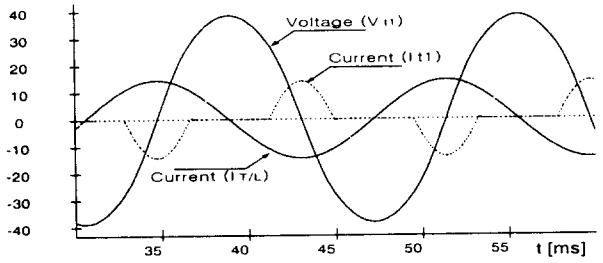

(a) The capacitor voltage, the reactor current (×10) and the transmission line current(×5)

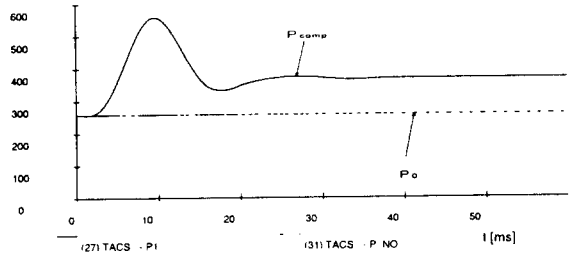

(b) The uncompensated real power flow P_o and the compensated real power flow, P_{comp}

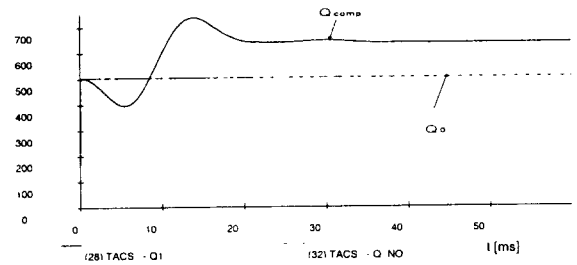

(c) The uncompensated reactive power flow Q_o and the compensated reactive power flow, Q_{comp}

Fig. 4 Waveforms of the single module TCSC system in the capacitive Vernier mode (σ = 80°)

The waveforms of Fig. 5 correspond with those of Fig. 4 except the thyristor conduction angle σ=160° , transmitting P_{comp}=90[W] and Q_{comp}= 228[Var] from the voltage source E_1 to the voltage source E_2, which means the effective impedance of the TCSC module inductive. The transient response, caused by the insertion of the inductive TCSC module, is also damped well, although somewhat oscillatory.

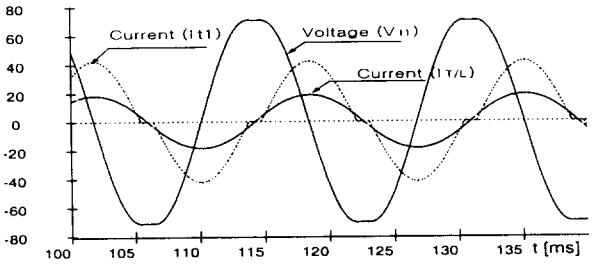

(a) The capacitor voltage, the reactor current(×5) and the transmission line current(×20)

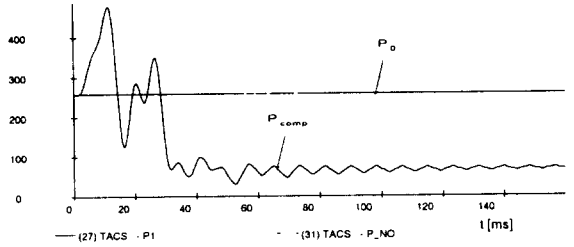

(b) The uncompensated real power flow P_o and the compensated real power flow, P_{comp}

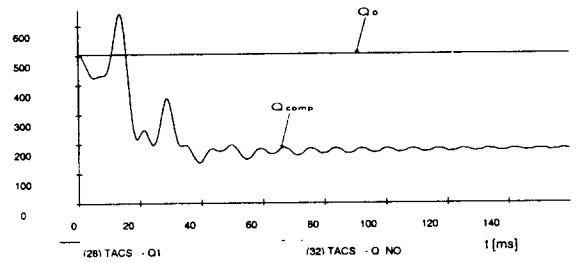

(c) The uncompensated reactive power flow Q_o and the compensated reactive power flow, Q_{comp}

Fig. 5 Waveforms of the single module TCSC system in the inductive Vernier mode (σ = 160°)

Fig. 6 shows the waveforms of the single-module TCSC power transmission system, transmitting P_{comp}=800[W] from the voltage source E_1 to the voltage source E_2 in the single-module TCSC power transmission system with σ =125° and φ=138° obtained by the load flow calculation. The first overshoot in the real power flow has the same magnitude as that shown in Fig. 4(b), which is for the capacitive operation of the Vernier mode TCSC module. However, moving to its new operating point in Fig. 6(a) takes longer time than in Fig. 4(b).

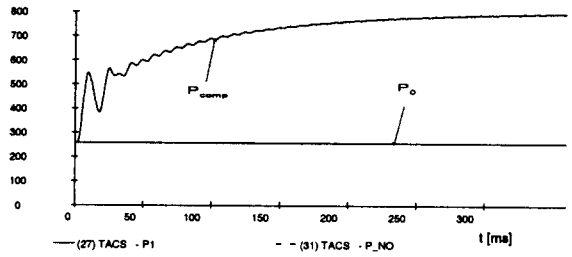

(a) The uncompensated real power flow P_o and the compensated real power flow, P_{comp}

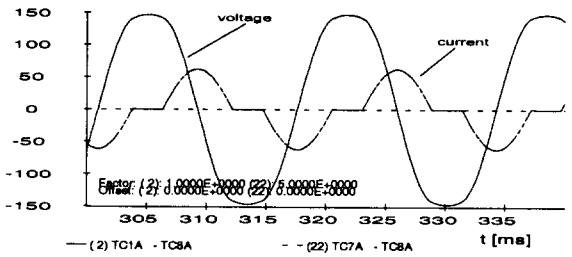

(b) The capacitor voltage and the reactor current(×5) of Vernier mode TCSC module

Fig. 6 Waveforms of the single module TCSC system in capacitive mode (σ = 125°)

Fig. 7(a) shows the transient response of real power flow, P_{comp}, after inserting the combination of the Vernier mode TCSC module with σ=80° and the blocked mode TCSC module to the simple power transmission system. Comparing to Fig. 4(b), which is for the single module TCSC with the conduction angle σ = 80° , the combined operation of the two-module TCSC can transmit the real power more than that of the single-module TCSC after brief transient overshoots. Fig. 7(b) shows the capacitor voltage and the reactor current of the Vernier mode TCSC module of the two-module TCSC power transmission system. The magnitudes of the voltage and the current of the Vernier mode TCSC are approximately close to those of Fig. 4(a).

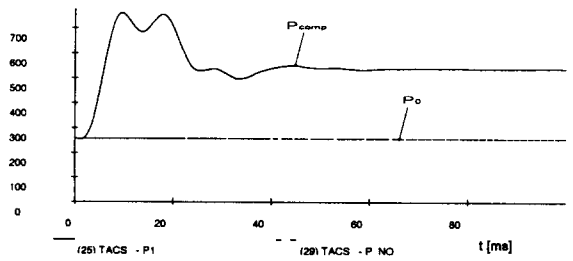

(a) The uncompensated real power flow P_o and the compensated real power flow, P_{comp}

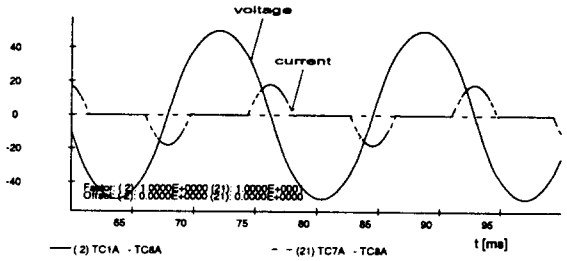

(b) The capacitor voltage and the reactor current(×10) of Vernier mode TCSC module

Fig. 7 Waveforms of the combined operation of Vernier mode (σ = 80°) and Blocked mode (σ = 0°)

Fig. 8(a) shows the transient response of real power flow from the voltage source E_1 to the voltage source E_2 after the insertion of the combination of the Vernier mode TCSC module with σ= 111° and the blocked mode TCSC module in the simple power transmission system. P_{comp} is set to 800[W] which equals the real power flow in Fig. 6(a). Comparing to the waveforms of Fig. 6(a), the transient overshoot of the two-module operation is shorter than that of one-module operation, which means the multi-module is capable of faster response. Fig. 8(b) shows the capacitor voltage and the reactor current of the Vernier mode TCSC module, which are smaller than those of Fig. 6(b). It means that the required ratings of each TCSC for the multi-module TCSC operation are smaller than those of the single-module TCSC operation.

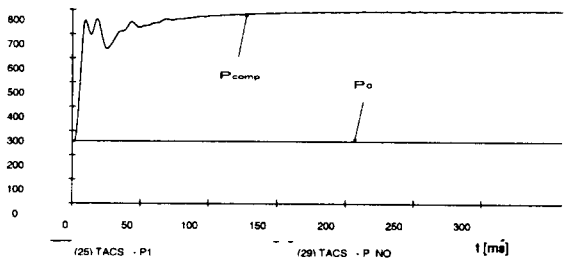

(a) The uncompensated real power flow P_o and the compensated real power flow, P_{comp}

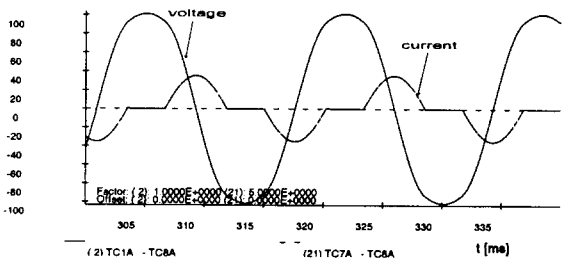

(b) The capacitor voltage and the reactor current(×5) of the Vernier mode TCSC module

Fig. 8 Waveforms of the combined operation of Vernier mode (σ = 111°) and Blocked mode (σ = 0°)

Fig. 9 shows the waveforms of the combined operation of the Vernier mode TCSC module with σ= 164° and the full conduction mode TCSC module, transmitting P_{comp}=90 [W], which equals the real power flow in Fig. 5(b). The effective impedance of the two-module TCSC is inductive. The transient overshoot of the real power flow of the two-module operation lasts longer and more oscillatory than those of Fig. 5(b), which is predicted by the magnitude of eigenvalues in Fig. 3(c). It means that the two-module TCSC working in the inductive compensation region does not control the real power flow more effectively than the single module TCSC. Fig. 9(b) shows the capacitor voltage and the reactor current of the Vernier mode TCSC module of the two-module TCSC power transmission system. Comparing Fig. 9(b) to Fig. 5(a) shows that the ratings of the two-module TCSC working at the inductive operating point are approximately equal to those of the single module TCSC working at the same operating point.

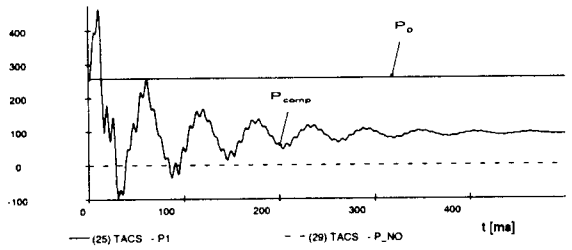

(a) The uncompensated real power flow P_o and the compensated real power flow, P_{comp}

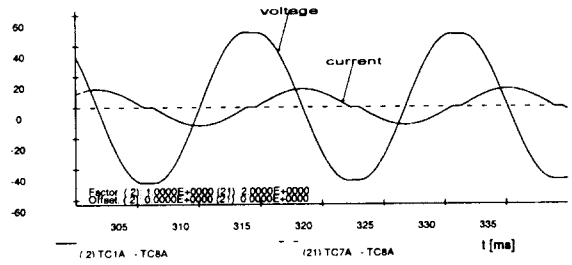

(b) The capacitor voltage and the reactor current(×2) of the Vernier mode TCSC module

Fig. 9 Waveforms of the combined operation of Vernier mode (σ= 164°) and Full conduction mode (σ= 180°)

5. Conclusion

In this paper, the load flow calculation, the stability analysis and the EMTP simulation of a TCSC power transmission system are performed to investigate the operating-mode characteristics of two-module TCSC as an equivalent of the multi-module TCSC.

The load flow calculation using the complex Fourier series representation of the switching function for the operation of thyristors informs the real and reactive power flows and the phase angle of the gating signals in the TCSC power transmission system. Results of the load flow calculation agree with results of the EMTP simulation.

Comparing to the Vernier mode operation of single-module TCSC in the power transmission system, two-module TCSC operation increases the real power flow with faster and smoother transient response and requires smaller ratings of the TCSC components. However, the transient response of two-module TCSC to decrease the real power flow shows greater overshoot and longer settling time, which are predicted by the stability analysis.

It may be concluded that two-module TCSC in a power transmission system as a real power flow controller shows better performance in the capacitive compensation region and less performance in the inductive compensation region than single-module TCSC. It is also concluded that the multi-module TCSC system should be carefully designed since the multi-module TCSC system is a mixture of TCSC modules, which each have their own operating mode.

Appendix 1

The parameters of the TCSC power transmission system in Fig. 1 are ;

$L_{t1} = L_{t2} = 20$ mH , $C_{t1} = C_{t2} = 244$ uF

$R_{t1} = R_{t2} = 10^{-3}$ Ω, $L_{T/L} = 153$ mH , $R_{T/L} = 10$ Ω

$E_1 = 170 \cdot \cos(377 \cdot t + 30°)$, $E_2 = 60 \cdot \cos(377 \cdot t - 10°)$.

Appendix 2

Table 1 Results of the load flow calculation.

Condition	P[W]	Q [Var]	φ	σ
Without TCSC	257	503	-	-
Single Module TCSC (Fig.4)	369.2	637	169.7°	80°
Single Module TCSC (Fig.5)	90	228	-41.5°	160°
Single Module TCSC (Fig.6)	800	968	138°	125°
Two Module TCSC (Blocked Mode) (Fig.7)	538	504	165°	80°
Two Module TCSC (Blocked Mode) (Fig.8)	800	968	144.5°	111°
Two Module TCSC (Full Conduction) (Fig.9)	90	228	-43.6°	164°

P : Real power flow flowing from E_1 in Fig. 1

Q : Reactive power flow flowing from E_1 in Fig. 1

φ : Phase angle of thyristor gate-firing signal

σ : Magnitude of thyristor conduction angle

Appendix 3

The system matrix, A, and the constant matrix, B, and the projection matrix, P_{rjt}, for the combined operation of a blocked mode TCSC module and a Vernier mode TCSC module in the simple power transmission system are written as

$$A = \begin{bmatrix} -\frac{R_{T/L}}{L_{T/L}} & 0 & -\frac{1}{L_{T/L}} & -\frac{1}{L_{T/L}} \\ 0 & -\frac{R_{t2}}{L_{t2}} & \frac{1}{L_{t2}} & 0 \\ \frac{1}{C_{t2}} & -\frac{1}{C_{t2}} & 0 & 0 \\ \frac{1}{C_{t1}} & 0 & 0 & 0 \end{bmatrix} \quad \text{(A-1)}$$

$$B = [\ \frac{1}{L_{T/L}},\ 0,\ 0,\ 0,\ ]^T \quad \text{(A-2)}$$

$$P_{rjt} = \begin{bmatrix} 1 & 0 & 0 & 0 \\ 0 & 0 & 0 & 0 \\ 0 & 0 & 1 & 0 \\ 0 & 0 & 0 & 1 \end{bmatrix} \quad \text{(A-3)}$$

Appendix 4

The system state vector, X(t), the system matrix, A, the constant matrix, B, and the projection matrix, P_{rjt}, of the combined operation of a full conduction mode TCSC module and a Vernier mode TCSC module are written as

$$X(t) = [\ I_{T/L}(t),\ I_{t1}(t),\ I_{t2}(t),\ V_{t1}(t),\ V_{t2}(t)\ ]^T \quad \text{(A-4)}$$

$$A = \begin{bmatrix} -\frac{R_{T/L}}{L_{T/L}} & 0 & 0 & -\frac{1}{L_{T/L}} & -\frac{1}{L_{T/L}} \\ 0 & -\frac{R_{t1}}{L_{t1}} & 0 & \frac{1}{L_{t1}} & 0 \\ 0 & 0 & -\frac{R_{t2}}{L_{t2}} & 0 & \frac{1}{L_{t2}} \\ \frac{1}{C_{t1}} & -\frac{1}{C_{t1}} & 0 & 0 & 0 \\ \frac{1}{C_{t2}} & 0 & \frac{1}{C_{t2}} & 0 & 0 \end{bmatrix} \quad \text{(A-5)}$$

$$B = [\ \frac{1}{L_{T/L}},\ 0,\ 0,\ 0,\ 0\ ]^T \quad \text{(A-6)}$$

$$P_{rjt} = \begin{bmatrix} 1 & 0 & 0 & 0 & 0 \\ 0 & 1 & 0 & 0 & 0 \\ 0 & 0 & 0 & 0 & 0 \\ 0 & 0 & 0 & 1 & 0 \\ 0 & 0 & 0 & 0 & 1 \end{bmatrix} \quad \text{(A-7)}$$

References

[1] E.V. Larsen, et. al., "Characteristics and Rating Considerations of Thyristor Controlled Series Compensation," IEEE PES Paper 93-SM-433-3-PWRD. Vancouver, British Columbia, July 1993.

[2] J. Urbanek, R.J. Piowko, E.V. Larsen, et al, " Thyristor Controlled Series Compensation Prototype Installation at the Slatt 500kV Substation," IEEE PES paper 92-SM-467-1 PWRD, Seattle, July 1992.

[3] S.G. Jalali and R.H. lasseter, "Harmonic Instabilities in Advanced Series Compensators," EPRI FACTS Conference, Boston, December, 1992, pp.1.4.3-1.4.28.

[4] S.G. Jalali, I. Dobson and R.H. lasseter, "Instabilities due to Bifurcation of Switching Times in a Thyristor Controlled Reactor," Proceedings of IEEE PESC'92, pp546-552.

[5] G.B. Chung et. al., "Analysis of the Operation of Thyristor Controlled Series Compensator interacting with Power System Components," in Proceeding of ITC_CSCC , pp. 741-744. Seoul, July 1996.

[6] F. Verhulst, "Nonlinear Differential Equations and Dynamical Systems," Springer-Verlag, Berlin, 1990.

저 자 소 개

정 교 범(鄭 敎 範)

1959년 12월 20일생, 1983년 서울대 공대 전기공학과(학사), 1985년 동 대학원 전기공학과(석사), 1992년 Univ. of Florida (공박), 1992년-1993년 Virginia Tech(Post Doc.), 1993년-1995년 한국전기연구소 선임연구원, 1995년~현재 홍익대 전자·전기·컴퓨터공학부 조교수

Tel : (0415) 860-2595

E-mail : gbchung@wow.hongik.ac.kr